2018 IEEE International Conference on Robotics and Automation (ICRA)
May 21-25, 2018, Brisbane, Australia

Emulating a Fully Actuated Aerial Vehicle using Two Actuators

James Paulos, Bennet Caraher, and Mark Yim

Abstract— **Micro air vehicles exemplified by quadrotors generate downward thrust in their body fixed frame and may only maneuver spatially by changing their orientation. As a result of this underactuation they are fundamentally incapable of simultaneously regulating orientation and position. Furthermore, their feasible maneuvers are limited to spatial trajectories with continuously differentiable acceleration. We present a coaxial helicopter which emulates full actuation over forces and torques (six degrees of freedom) using only two actuators. The orientation of the thrust vector from each rotor is governed by the drive motor by exciting a cyclic flapping response in special articulated blades. The useful separation of orientation and translation dynamics is demonstrated in flight experiments by tracking spatial trajectories while maintaining flat body attitude as well as tracking desired orientations near hover while station keeping.**

I. INTRODUCTION

A variety of micro air vehicle (MAV) technologies are now available which provide the fundamental flight capabilities required for basic survey and transport tasks. These aircraft exhibit highly coupled rotational and lateral dynamics which must be taken into account in the control design and when specifying aggressive required trajectories. A popular example is the planar quadrotor, whose flight state exists in six dimensions over position and body orientation but which is equipped with only four actuators. These aircraft only have control over their attitude moment vector and the magnitude of net thrust downward in the body frame, and so they must maneuver spatially by constantly changing their orientation. As a direct consequence of this underactuation they are incapable of independently regulating both position and orientation. Furthermore, even smooth spatial trajectories can be infeasible unless they are c^3, which excludes such common techniques as both minimum jerk and trapezoidal velocity multi-segment trajectories.

Fully actuated aircraft with independent control over body forces and moments could support a multitude of new capabilities. Such aircraft would be able to apply arbitrary wrenches on the environment, making them useful for construction or object manipulation. In flight they could independently point cameras, sensors, or high gain antennas independent of motion trajectories or the wind environment. In indoor environments with humans they would able to gesture with the aircraft posture to make their motion intentions more legible to bystanders, visually indicate objects or directions as a guide, or provide visual cues to aid in human-robot task coordination. These possibilities have inspired diverse efforts to realize new types of fully actuated MAV.

Many previous embodiments of fully actuated, holonomic, or omnidirectional MAV are conceptually inspired by the quadrotor and proceed by adding additional actuators. By configuring six conventional rigid rotors with their orientations canted out of plane it is possible to obtain independent control over forces and moments in proximity to hover, but the inability to reverse independent rotor thrust directions limit feasible forces and therefore feasible stable orientations [1], [2]. With seven unidirectional rotors it becomes in principle possible to hover in all orientations, even upside down [3]. Incorporating eight variable-direction rotors allows practical flight in all orientations and would potentially permit control strategies which avoid driving motors at low speeds or with rapid direction changes [4]. Similar capabilities in six-rotor configurations become possible with high performance reversing motor drivers [5].

Coaxial helicopters offer a different point of departure for developing fully actuated aircraft. One technique is to vector the thrust of top and bottom rotors by reorienting the entire motor and rotor assembly using gimbals driven by additional pitch and roll servomotors. In static bench testing, [6] demonstrated that the resulting six-actuator system can obtain authority over net forces and moments. Alternatively, a pair of conventional swashplates and teetering rotors can be driven by four roll and pitch servos to tilt the rotor tip path plane and achieve a similar effect. Conventional flight capabilities using this technique were obtained by [7], but novel maneuvers unique to fully actuated MAV were not deeply explored. Both types of coaxial aircraft have an efficiency advantage over the aforementioned multirotors in that all of the rotor thrust can be directed downwards when in hover. However, each still require a minimum of six actuators for operation.

This paper introduces a new coaxial helicopter which emulates fully actuated aircraft using only two actuators. We do this by taking advantage of recent methods for controlling a flapping rotor's tip path plane by exciting a dynamic response to modulated shaft torques from the primary drive motor [8], [9]. Section II describes the idealized vehicle dynamics in terms of vectored thrusts derived from tilting top and bottom rotor tip path planes. Our method for controlling the tip path plane response without auxiliary actuators is described in Section III along with measurements of the individual rotor capabilities. The vehicle hardware design is summarized in Section IV, and the control architecture is de-

This work was supported through NSF Grant No. 1138847.

The authors are with the Dept. of Mech. Eng. & Appl. Mechanics and GRASP Lab at the University of Pennsylvania, Philadelphia, PA. {jpaulos,bcaraher,yim}@seas.upenn.edu

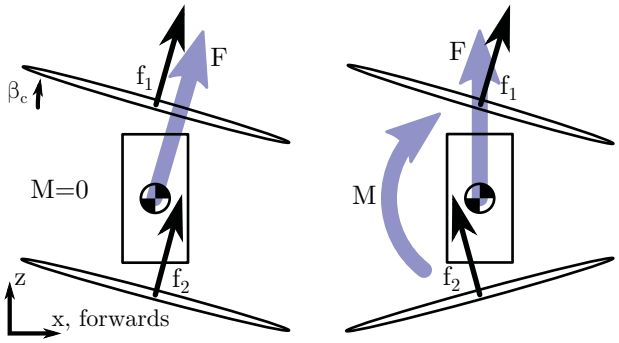

Fig. 1. Teetering rotors allow independent control of force and moments.

scribed in Section V. Flight results in Section VI demonstrate decoupled lateral and rotational dynamics, confirming that this two-actuator MAV emulates the primary capabilities of a six-actuator, fully actuated MAV. This includes sustaining a stationary hover while pitching the aircraft up to $8°$, and tracking trajectories with discontinuous accelerations up to $1\,\mathrm{m/s^2}$ without pitching or rolling. We conclude by identifying areas for improvement and future work.

II. IDEALIZED VEHICLE DYNAMICS

The vehicle dynamics can be approximated by considering a coaxial helicopter capable of tilting the direction of thrust from each rotor away from vertical. This thrust vectoring effect could conventionally be obtained from teetering rotors equipped with cyclic blade pitch control actuators. Our unique method for controlling the blade response using only the main drive torque will be examined in Section III, but first we address a generic thrust vectoring idealization. Figure 1 depicts one rotor mounted a distance r_1 above the center of mass and a second counter rotating rotor mounted a distance r_2 below the center of mass. The figure conceptually illustrates that the force vectors f_1 and f_2 can be directed counter to each other in order to produce a net pitching moment about the vehicle's center of mass while maintaining zero net lateral force. Alternatively, the force vectors can be pointed in similar directions, yielding a net lateral force on the aircraft while maintaining zero net moment.

Equation 1 develops the net force F and moment M vectors about the aircraft center of mass as a linear function of the individual rotor force vectors f_1 and f_2. In addition to these rotor forces, we model a corresponding reaction torque about the z axis for each rotor which is proportional to its thrust along the z axis by a constant coefficient k_Q. This is a reasonable approximation for the small angular deflections in the forces considered here. Vectors F, M, f_1, and f_2 are written in component form in Eq. 1 with respect to body fixed x, y, and z axes.

$$\begin{bmatrix} F_x \\ F_y \\ F_z \\ M_x \\ M_y \\ M_z \end{bmatrix} = \begin{bmatrix} 1 & 0 & 0 & 1 & 0 & 0 \\ 0 & 1 & 0 & 0 & 1 & 0 \\ 0 & 0 & 1 & 0 & 0 & 1 \\ 0 & -r_1 & 0 & 0 & r_2 & 0 \\ r_1 & 0 & 0 & -r_2 & 0 & 0 \\ 0 & 0 & -k_Q & 0 & 0 & k_Q \end{bmatrix} \begin{bmatrix} f_{1x} \\ f_{1y} \\ f_{1z} \\ f_{2x} \\ f_{2y} \\ f_{2z} \end{bmatrix} \quad (1)$$

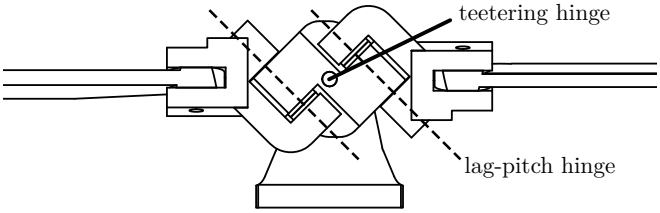

Fig. 2. Teetering rotor with skewed lag-pitch hinges.

The constant coefficient matrix has a determinant of $2k_Q(r_1 + r_2)^2$ and so will be full rank and invertible so long as the two rotors are not co-located. As a result the relationship can be inverted, and Eq. 2 provides a unique solution for allocating individual rotor controls f_1 and f_2 given a desired net vehicle force and moment. If the six components of rotor forces f_1 and f_2 are available as independent inputs, the aircraft will be fully actuated in all six operational degrees over orientation and position.

$$\begin{bmatrix} f_{1x} \\ f_{1y} \\ f_{1z} \\ f_{2x} \\ f_{2y} \\ f_{2z} \end{bmatrix} = \begin{bmatrix} \frac{r_2}{r_1+r_2} & 0 & 0 & 0 & \frac{1}{r_1+r_2} & 0 \\ 0 & \frac{r_2}{r_1+r_2} & 0 & \frac{-1}{r_1+r_2} & 0 & 0 \\ 0 & 0 & \frac{1}{2} & 0 & 0 & -\frac{1}{2k_Q} \\ \frac{r_1}{r_1+r_2} & 0 & 0 & 0 & \frac{-1}{r_1+r_2} & 0 \\ 0 & \frac{r_1}{r_1+r_2} & 0 & \frac{1}{r_1+r_2} & 0 & 0 \\ 0 & 0 & \frac{1}{2} & 0 & 0 & \frac{1}{2k_Q} \end{bmatrix} \begin{bmatrix} F_x \\ F_y \\ F_z \\ M_x \\ M_y \\ M_z \end{bmatrix} \quad (2)$$

III. IMPLEMENTATION OF THRUST VECTORING

Thrust vectoring for control through tilting of the tip path plane can be implemented without adding any additional actuators beyond the top and bottom drive motors themselves. In previous work it has been shown that a single motor can control both the mean operating speed and cyclic blade pitch variation of a rotor by modulating the applied drive torque [8]. Two blades are attached to a hub with skewed lag-pitch hinges, as shown in Fig. 2. Modulating the motor torque sinusoidally at one-per-rev excites a synchronous lead-lag motion in each blade within the plane of rotation. The skewed lag-pitch hinge couples this lag oscillation into a blade pitch oscillation. The two blades are mounted on asymmetric hinges so that one has a positive lag-pitch coupling and the other a negative lag-pitch coupling. As a result a one-per-rev sinusoidal modulation in motor torque causes the blades to pitch $180°$ out of phase with each other, phase locked with the rotor rotation. By controlling the amplitude and phase of the motor torque the amplitude and azimuthal phase of the blade pitch can be controlled. The aircraft in [8] is capable of attitude control like a standard quadrotor or helicopter and maneuvers by taking advantage net direct hub moments arising when, for example, both blades cyclically pass across the aircraft nose at minimum pitch and lift but pass across the tail at maximum pitch and lift.

Independent offset flap hinges were added in [9] to allow each blade to individually flap up and down during each revolution in response to changing blade pitches and the resulting blade lift. In addition to direct moments on the

hub, this causes an apparent tilting of the tip path plane and redirection of the thrust vector.

The operational principle depicted in Fig. 1 benefits from large flapping angles and a pure thrust vectoring effect with no direct moments applied to the hub, properties which neither of the rotor designs in [8] or [9] achieve. This is now obtained by incorporating a single, central teetering hinge as seen in Figs. 2 and 3. For each degree of cyclic blade pitch authority a teetering rotor enjoys one degree of flap and tip path plane inclination, and the thrust force may be thought of as remaining perpendicular to this tip path plane. At the same time, no direct torques can be transfered to the hub through the teetering hinge.

The change in blade flap angle β as a function of azimuthal angle ψ is conventionally described as

$$\beta(\psi) = \beta_c \cos(\psi) + \beta_s \sin(\psi) \tag{3}$$

where $\psi = 0$ in the aft direction and ψ increases in the direction of rotation. It follows that, for the counterclockwise top rotor, β_c describes a longitudinal tilting of the tip path plane forwards and β_s describes a lateral tilt towards the side of the retreating blade. The thrust can be expressed as a function of rotor speed Ω_1 and thrust coefficient k_T as $k_T\Omega_1^2$. Employing a small angle approximation in β the rotor force vectors f_1 and similarly constructed f_2 are expressed in Eq. 4, where the difference in sign is due to their opposing directions of rotation.

$$\begin{aligned} f_{1x} &= k_T\Omega_1^2\beta_c & f_{2x} &= k_T\Omega_2^2\beta_c \\ f_{1y} &= k_T\Omega_1^2\beta_s & f_{2y} &= -k_T\Omega_2^2\beta_s \\ f_{1z} &= k_T\Omega_1^2 & f_{2z} &= k_T\Omega_2^2 \end{aligned} \tag{4}$$

The motor torques driving the gross propeller rotation as well as the cyclic blade pitch and flapping response are a result of modulating the applied motor voltage. The applied voltage V is the sum of two parts: a proportional-integral control on error between the observed rotor speed $\dot{\psi}$ and desired speed Ω with gains k_P and k_I, and an additional voltage modulation $\tilde{V}$.

$$V = -k_P(\dot{\psi} - \Omega) - k_I \int (\dot{\psi} - \Omega)dt + \tilde{V} \tag{5}$$

Previous dynamical modeling and experimental validation of similar rotors in [9] motivates a useful approximation for the flap response in terms of the applied voltage modulation. The flap response in β lags the voltage modulation $\tilde{V}$ by an angle ϕ_β. The flap amplitude is proportional to the voltage amplitude $\tilde{V}$ in excess of a minimum threshold $\tilde{V}_{min}$ by a linear constant k_β. Parameters ϕ_β, $\tilde{V}_{min}$, and k_β are functions of the rotor physical properties, electromechanical motor properties, and software speed control gains. They are valid near a trim thrust condition, and are readily determined with a bench test. The final expression for $\tilde{V}$ is then given by Eq. 6, where it is convenient to write the desired flapping in terms of polar amplitude a and phase ϕ.

Fig. 3. Top rotor of coaxial helicopter.

Fig. 4. Coaxial helicopter.

$$\begin{aligned} a &= \sqrt{\beta_c^2 + \beta_s^2} \\ \phi &= \operatorname{atan2}(\beta_s, \beta_c) \\ \tilde{V} &= (\tilde{V}_{min} + k_\beta a)\cos(\psi - \phi - \phi_\beta) \end{aligned} \tag{6}$$

IV. HARDWARE DESIGN

The flight vehicle is shown in Fig. 4, incorporating two counter-rotating propeller systems which are depicted in Fig. 3. The rotors are $32\,\mathrm{cm}$ in diameter, and are driven to a trim hover speed of approximately $370\,\mathrm{rad/s}$ by two size 2212 BLDC motors. The rotor blades are commercial symmetric airfoils attached to custom 3D printed hub pieces which are joined by steel pin hinges with PTFE plastic washers added to reduce friction. The full aircraft mass is $380\,\mathrm{g}$, with the center of mass approximately equidistant between the two rotors which are themselves $16\,\mathrm{cm}$ apart.

A commercial flight controller using the PX4 autopilot software [10] runs an attitude tracking control law to generate desired body moments M. The desired body attitude as well as additional body force commands F are passed in through a WiFi radio link. The flight controller calculates speed Ω and flap parameters β_c, β_s for each rotor based on linear combinations of F and M consistent with Eqs. 2 and 4 near

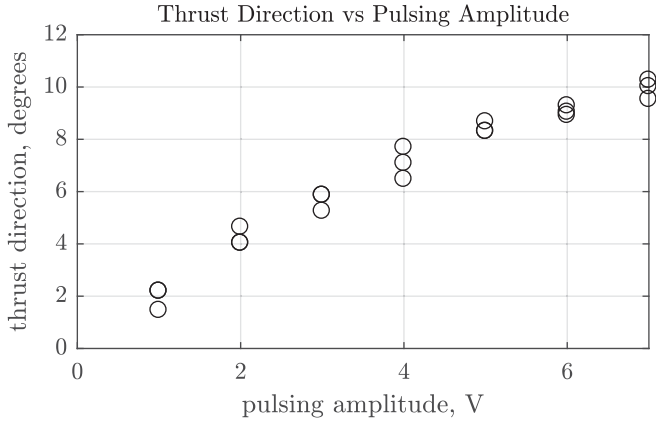

Fig. 5. Bench measurements of lateral forces and increasing voltage modulation amplitude.

trim. These parameters are passed to the motor controller as three PWM encoded values.

The custom motor controller is responsible for applying drive voltage V based on desired parameters Ω, β_c, and β_s according to Eq. 5 and 6. This is made possible by direct measure of the hub orientation ψ using a 4096 count hall effect rotary encoder.

During bench testing the rotor was operated at $370\,\mathrm{rad/s}$, obtaining a thrust of $2.9\,\mathrm{N}$. Figure 5 shows the obtained angular deflection of the thrust vector due to blade flapping as determined by measuring the lateral forces generated. These angles agree closely with a visual observation of the tip path plane. A maximum deflection of 10° in the force vector was obtained, corresponding to a lateral force of $0.5\,\mathrm{N}$.

V. CONTROL DESIGN

Trajectory tracking control for a conventional underactuated quadrotor might proceed as illustrated in Fig. 6 using cascaded position and attitude controllers. A reference spatial trajectory x_t is compared with the observed vehicle position x and desired corrective accelerations $\ddot{x}_{des}$ are computed. An attitude planner identifies a desired vehicle orientation R_{des} and thrust T_{des} associated with that acceleration, and a closed loop attitude controller generates desired body moments M_{des} to track the commanded orientation. The desired thrust T_{des} and moment M_{des} are passed through an approximate inverse actuator model to produce low level actuator commands u (e.g. rotor speeds). Those commands produce aerodynamic forces and moments F and M for the physical aircraft, which responds subject to its dynamics.

In contrast, the updated control architecture in Fig. 7 takes advantage of the fully actuated capabilities of the new aircraft. The desired orientation R_{des} can be freely specified as part of the trajectory alongside x_t. Desired translational accelerations $\ddot{x}_{des}$ can be expressed in the body frame directly as desired forces F_{des}. Desired forces and moments F_{des}, M_{des} are transformed by the inverse actuator model given by Eq. 2 into low level actuator commands Ω, β_c, and β_s representing the speed and tip path plane tilt for each rotor.

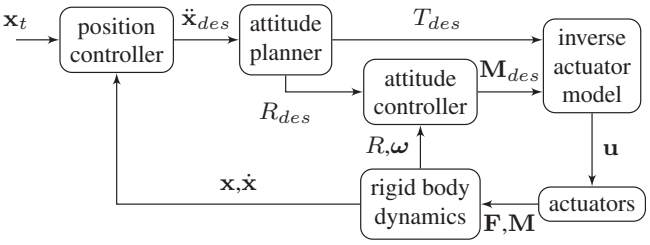

Fig. 6. Conventional trajectory control for underactuated quadrotor.

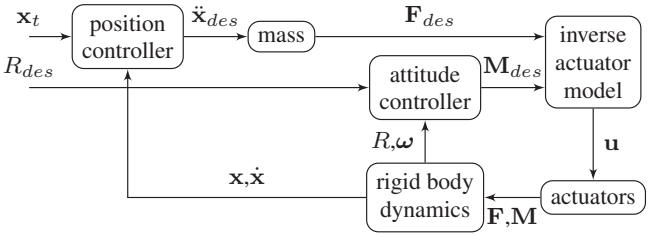

Fig. 7. Fully actuated trajectory and orientation control.

VI. FLIGHT EXPERIMENTS

Three different flight experiments were conducted to demonstrate full actuation of aircraft moments and forces, separation of rotational and translational dynamics, and the impact of actuator limitations on the available flight envelope. In each flight the aircraft tracks a time parameterized trajectory in simultaneous orientation and position. The attitude tracking controller and actuator control allocation are performed on the aircraft using onboard sensor information. The position controller is implemented on a ground based laptop which makes use of absolute position and heading information available from a motion capture system. The resulting force commands sent to the vehicle reflect both proportional-derivative action and the reference acceleration of the target trajectory.

A. Orientation Control in Hover

In the first experiment the aircraft ascends to a stable hover at position $(x, y) = (0, 0)$. The aircraft then pitches nose down to -8° and then up to 8° while maintaining a stationary position error of less than $5\,\mathrm{cm}$ as shown in Fig. 8. Since the aircraft is stationary, the net force must be the aircraft weight $3.7\,\mathrm{N}$ directed 8° off the body fixed z axis, representing a lateral force in the body frame of $0.5\,\mathrm{N}$.

This test demonstrates the maximum pitch angle at which the vehicle can remain stationary. At larger pitch angles there is insufficient flapping authority to avoid accelerating in the direction of the aircraft pitch. Since this experiment establishes that the vehicle can produce $0.5\,\mathrm{N}$ lateral force in hover, one might expect a theoretical maximum lateral acceleration of $1.3\,\mathrm{m/s^2}$ even while maintaining perfect level pitch, which is analogous to the acceleration of a quadrotor pitched over at 8°.

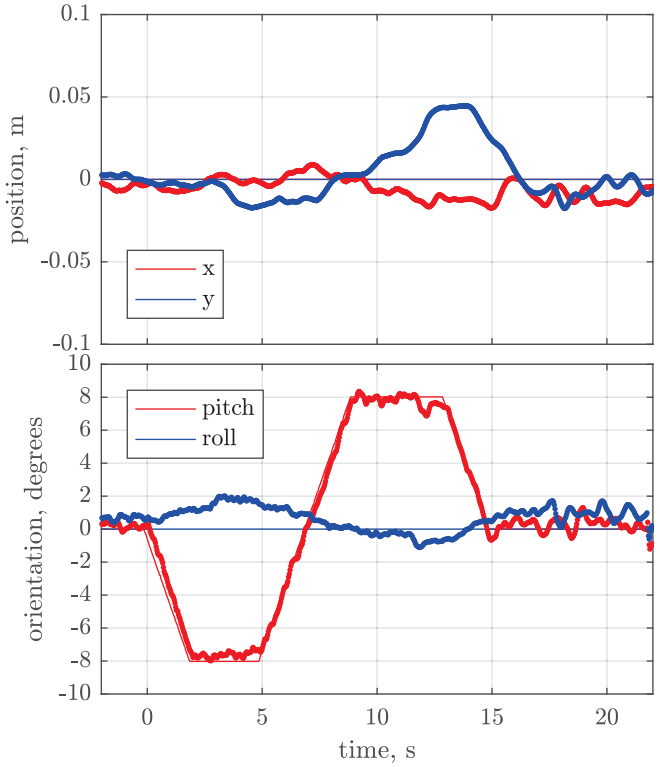

Fig. 8. Stationary hover while pitching from $-8°$ to $8°$.

B. Acceleration without Pitch or Roll

The experiment described in Fig. 9 demonstrates tracking a trajectory which would be very challenging for an underactuated quadrotor to execute accurately. Furthermore, the aircraft maintains a level attitude throughout the maneuver which would be impossible for a quadrotor. From rest in hover, the commanded lateral acceleration steps instantaneously to $1\,\mathrm{m/s^2}$. The velocity increases uniformly until the aircraft reaches $1\,\mathrm{m/s}$, at which time the acceleration instantaneously becomes zero again. After cruising some distance at constant speed the vehicle speed is then arrested with a period of constant deceleration at $1\,\mathrm{m/s^2}$. Figure 9 shows that the vehicle faithfully tracks the trapezoidal velocity profile. Because the tip path plane dynamics are so much faster than the body attitude dynamics of a quadrotor, it can even do a fair job tracking the instantaneous step in acceleration which, for a quadrotor, would require instantaneous reorientation of the entire vehicle. Meanwhile the vehicle remains within approximately $1°$ of a flat hover posture throughout the maneuver, while a quadrotor would be forced to pitch to more than $5°$ to achieve similar acceleration.

C. Smooth Trajectory Following

Many apparently smooth trajectories which might be desired by camera operators or generated by spline methods are likewise difficult for an underactuated MAV to execute cleanly. Figures 10 and 11 show the MAV flying at $0.5\,\mathrm{m/s}$ and then entering tangentially into a circular path of radius

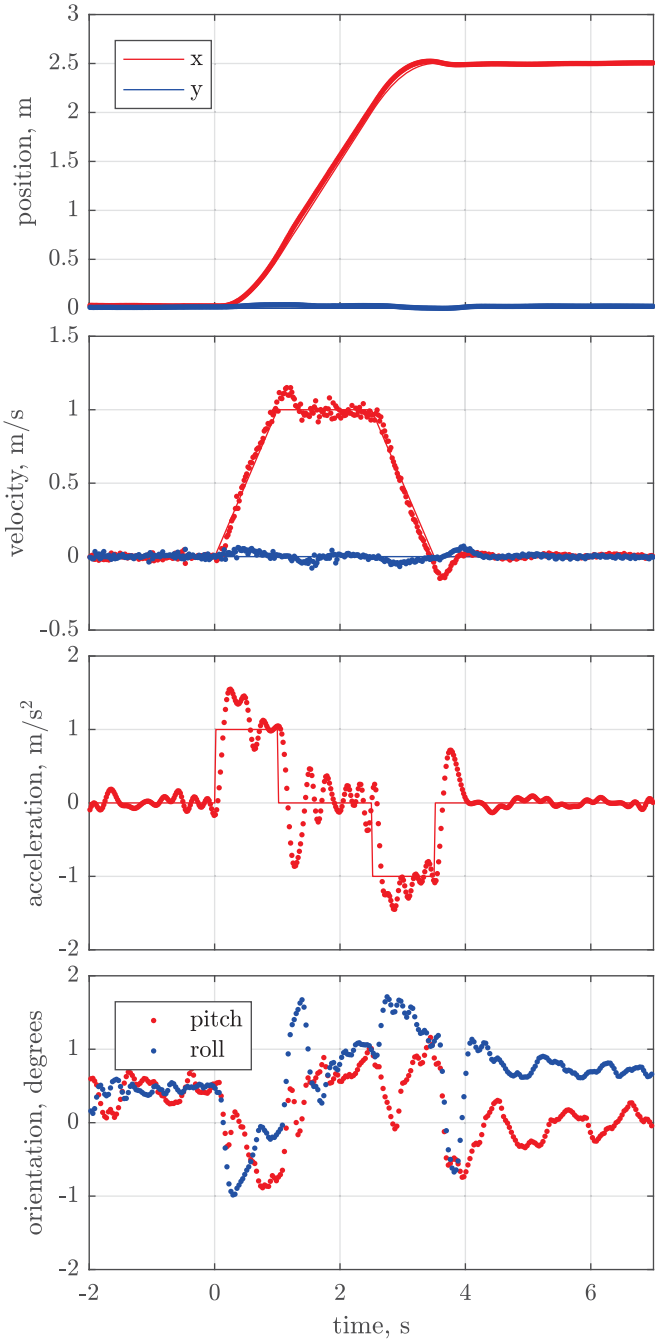

Fig. 9. Acceleration at $1\,\mathrm{m/s^2}$ while maintaining flat attitude.

$35\,\mathrm{cm}$. Upon entry into the circle, the required acceleration jumps from $0\,\mathrm{m/s^2}$ to $0.7\,\mathrm{m/s^2}$. Then as the circle is tracked while maintaining heading in the x direction the acceleration vector continuously changes direction in both the world and body frames. Once again this maneuver can be completed with approximately $1°$ of unwanted pitching and rolling of the aircraft.

VII. CONCLUSION

This work presents the design and flight testing of a coaxial helicopter with only two actuators which can emulate

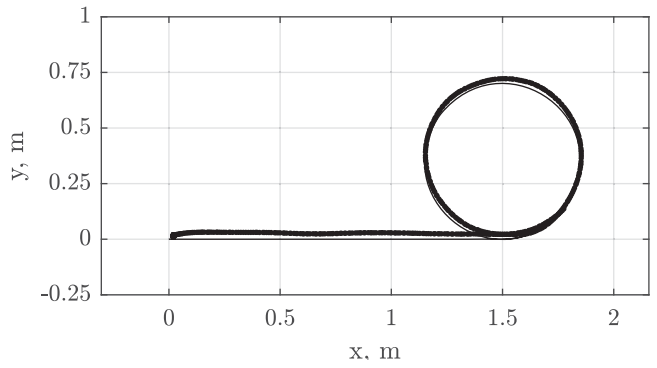

Fig. 10. Flight at 0.5 m/s into a circle of radius 35 cm.

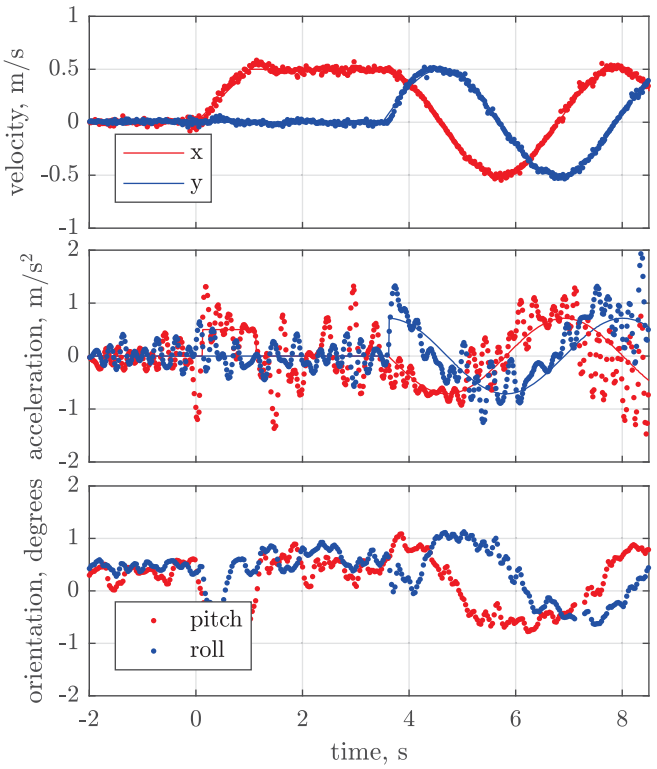

Fig. 11. Flight at 0.5 m/s into a circle of radius 35 cm.

the capabilities of a fully actuated MAV. Unlike a conventional underactuated quadrotor this MAV enjoys independent control over the body moment and force vectors, making it possible to hover in non-upright orientations or accelerate laterally without pitching or rolling the aircraft. Similar capabilities in the past have only been achieved using a total of six or more actuators. Experiments demonstrate the ability to maintain a stationary hover while pitched at up to 8°, as well as the ability to accelerate laterally at 1 m/s^2 without pitching or rolling. Since the aerodynamic force is directed by fast rotor flapping dynamics instead of relying on changing the attitude of the entire aircraft, even smooth trajectories with discontinuous required accelerations can be tracked with a high degree of fidelity.

Existing platforms overcome the limitations of underactuated flight dynamics by adding articulated subsystems. Conventional quadrotors can not fully control their body wrench, but they can be equipped with a dexterous manipulator to apply wrenches to grasped objects. The view from a rigidly mounted camera suffers uncontrollable rolling and pitching during flight maneuvers, but cameras can be mounted on multi-axis gimbals. Embedding these capabilities directly into the flight platform itself may allow for lighter, cheaper and more robust MAV.

Future work will focus on increasing the angle of thrust vectoring available from each rotor. This will expand the permissible orientations for hover and increase the feasible lateral forces and accelerations for tracking trajectories or rejecting wind disturbances. The aerodynamic interaction between the rotors has been ignored in the present work. Modeling these effects may inform the design of the top and bottom rotors for improved aerodynamic efficiency or suggest modified command allocations for more accurately generating desired forces and moments. Finally, we have considered only the situation where both aircraft orientation and path are simultaneously prescribed. Returning to the classic problem of tracking aggressive spatial trajectories, we may consider how to optimally exploit both the free attitude dynamics and force vectoring capabilities subject to actuator constraints.

References

[1] B. Crowther, A. Lanzon, M. Maya-Gonzalez, and D. Langkamp, "Kinematic analysis and control design for a nonplanar multirotor vehicle," *Journal of Guidance, Control, and Dynamics*, vol. 34, no. 4, pp. 1157–1171, 2011.

[2] G. Jiang and R. Voyles, "Hexrotor UAV platform enabling dextrous interaction with structures - flight test," in *2013 IEEE International Symposium on Safety, Security, and Rescue Robotics (SSRR)*, Oct. 2013, pp. 1–6.

[3] A. Nikou, G. C. Gavridis, and K. J. Kyriakopoulos, "Mechanical design, modelling and control of a novel aerial manipulator," in *2015 IEEE International Conference on Robotics and Automation (ICRA)*, May 2015, pp. 4698–4703.

[4] D. Brescianini and R. D'Andrea, "Design, modeling and control of an omni-directional aerial vehicle," in *2016 IEEE International Conference on Robotics and Automation (ICRA)*, May 2016, pp. 3261–3266.

[5] P. Boyle, C. Kobata, C. Liu, D. Shanks, and A. Weinstein, "Team Volonomic VI demo video," Apr. 2017.

[6] S. Prothin and J.-M. Moschetta, "A vectoring thrust coaxial rotor for micro air vehicle: Modeling, design and analysis," in *3AF, 48th International Symposium of Applied Aerodynamics*, Saint Louis, France, Mar. 2013.

[7] S. George and P. Samuel, "On the design and development of a coaxial nano rotorcraft," in *50th AIAA Aerospace Sciences Meeting*, Nashville, TN, Jan. 2012.

[8] J. Paulos and M. Yim, "Flight performance of a swashplateless micro air vehicle," in *2015 IEEE International Conference on Robotics and Automation (ICRA)*, Seattle, WA, May 2015, pp. 5284–5289.

[9] J. Paulos and M. Yim, "Cyclic Blade Pitch Control Without a Swashplate for Small Helicopters," *Journal of Guidance, Control, and Dynamics*, vol. 41, no. 3, pp. 689–700, 2018.

[10] L. Meier, D. Honegger, and M. Pollefeys, "PX4: A node-based multithreaded open source robotics framework for deeply embedded platforms," in *2015 IEEE International Conference on Robotics and Automation (ICRA)*, May 2015, pp. 6235–6240.